Am J Cancer Res 2023;13(3):1067-1081
www.ajcr.us /ISSN:2156-6976/ajcr0149532

Original Article

IRG1/Itaconate induces metabolic reprogramming to suppress ER-positive breast cancer cell growth

Hsueh-Chun Wang[1,2], Wei-Chao Chang[2,3], Der-Yen Lee[4], Xing-Guo Li[1,2,5], Mien-Chie Hung[1,5]

[1]Graduate Institute of Biomedical Sciences, China Medical University, Taichung 406040, Taiwan; [2]Research Center for Cancer Biology, China Medical University, Taichung 406040, Taiwan; [3]Center for Molecular Medicine, China Medical University Hospital, China Medical University, Taichung 406040, Taiwan; [4]Graduate Institute of Integrated Medicine, China Medical University, Taichung 406040, Taiwan; [5]Institute of Biochemistry and Molecular Biology, China Medical University, Taichung 406040, Taiwan

Received February 6, 2023; Accepted March 1, 2023; Epub March 15, 2023; Published March 30, 2023

Abstract: Most breast cancers are estrogen receptor (ER)-positive, targeted by endocrine therapies, but chemoresistance remains a significant challenge in treating the disease. Altered intracellular metabolite has closely connected with the pathogenic process of breast cancer and drug resistance. Itaconate is an anti-inflammatory metabolite generated from converting cis-aconitate in the tricarboxylic acid (TCA) cycle by the immune response gene 1 (IRG1). However, the potential role of IRG1/Itaconate in the crosstalk of metabolic pathways and tumor development is currently unknown. We tested the hypothesis that IRG1/Itaconate controls metabolic homeostasis to modulate breast cancer cell growth. We showed that breast cancers harboring an IRG1 deletion displayed a worse prognosis than those without IRG1 deletion; approximately 70% of breast cancer with IRG1 deletion were ER-positive. There was no significant difference in the IRG1 copy number, mRNA, and protein levels between ER-positive and ER-negative breast cancer cell lines and breast tumors. Itaconate selectively inhibited ER-positive breast cancer cell growth via the blockade of DNA synthesis and the induction of apoptosis. Mechanistically, IRG1 overexpression led to decreased intermediate levels of glycolysis, the TCA cycle, and lipid metabolism to compromise the entire biomass and energy of the cell. Itaconate inhibited the enzymatic activity of succinate dehydrogenase (SDH) in the mitochondrial electron-transport chain, concomitant with reactive oxygen species (ROS) production and the decreased adenylate kinase (AK) activities, which, in turn, induced AMP-activated protein kinase (AMPK) activation to restore metabolic homeostasis. These results suggest a new regulatory pathway whereby IRG1/Itaconate controls metabolic homeostasis in ER-positive breast cancer cells, which may contribute to developing more efficacious therapeutic strategies for breast cancer.

Keywords: Breast cancer, estrogen receptor, immune response gene 1, itaconate, metabolic reprogramming, tricarboxylic acid cycle

Introduction

Over 70% of all breast cancers are estrogen receptor (ER)-positive [1], targeted by endocrine therapies, tamoxifen. While tamoxifen treatment reduces mortality by 31%, over half of the advanced ER-positive breast cancers are intrinsically resistant to tamoxifen, and about 40% acquired resistance during the treatment [2, 3]. Still, chemoresistance remains a significant challenge in the treatment of breast cancer.

Cancer cells often rewrite their biochemical pathways to adapt to increased metabolic stress from increased energy demand during tumorigenesis. This changing intracellular metabolites to meet energy demand and function as non-metabolic signals is essential for tumor development and progression [4-6]. The tricarboxylic acid (TCA)-derived intermediates are well-recognized oncometabolite that promote tumorigenesis via regulating chromatin modifications and DNA methylation [4-7]. Altered lipid metabolism has also closely connected with the pathogenic process [8-12]. Consequently, metabolic reprogramming fuels cell growth and contributes to cancer drug resistance [13, 14]. Revealing the key metabolites in tumorigenesis will provide a foundation

for developing alternative strategies targeting breast cancer.

Itaconate is an anti-inflammatory metabolite synthesized from cis-aconitate in the TCA cycle by immune response gene 1 (IRG1) [4, 15-22]. Large quantities of itaconate can be produced in activated murine macrophages, which block the release of proinflammatory cytokines and inhibit succinate dehydrogenase (SDH)-derived reactive oxygen species (ROS) production [17, 18, 23, 24]. Moreover, itaconate can alkylate kelch-like ECH-associated protein 1 (KEAP1) and glutathione (GSH), leading to activating the master antioxidant regulator, nuclear factor erythroid 2-related factor 2 (NRF2) [20] and inducing the anti-inflammatory transcriptional factor, activating transcription factor 3 (ATF3) [19], respectively. As itaconate is a cysteine-modifying compound, itaconate likely exerts other effects through unknown mechanisms to control cell functions. As a corollary, IRG1/Itaconate can alter TCA cycle metabolism and impacts branched-chain amino acid metabolism and fatty acid diversity, leading to changes in energy metabolism, mitochondrial function, and cell growth [23].

Bisphenol-A (BPA) exposure in utero has been linked to breast cancer and abnormal mammary gland development in mice [25]; the exposed mice showed significantly decreased IRG1 mRNA expression in mammary tissue [25]. Besides, dimethyl-itaconate, a membrane-permeable derivative, could reduce the high inflammatory state of ulcerative colitis and colitis-associated cancer risk in a mouse model [26], suggesting a link between itaconate in inflammation and tumorigenesis. The current study aimed to advance the direct role of the IRG1 gene and its enzymatic metabolite, itaconate, in tumor cell growth and breast cancer development.

This study hypothesized that the IRG1/Itaconate is crucial in determining ER-positive breast cancer cell fate and potentially therapeutically treating breast cancer. We discovered ER-positive breast cancer cells were more responsive to itaconate-induced cell death than ER-negative cells. IRG1/Itaconate caused cell cycle arrest via DNA proliferation inhibition and apoptosis due to the resulting energy stress. Mechanically, IRG1/Itaconate induced activation of the AMP-activated protein kinase (AMPK) pathway in response to metabolic stress, accompanied by the change in glycolysis, the TCA cycle, and the lipid metabolites. Consequently, IRG1/Itaconate triggered metabolic stress via metabolic reprogramming, leading to mitochondrial dysfunction and cell death in ER-positive breast cancer cells.

Materials and methods

Chemicals

Itaconate was purchased from Sigma-Aldrich, Inc., St. Louis, MO, USA. 4-Octyl-itaconate was purchased from Cayman Inc.

Cell culture and transfection

BT474 (ATCC HTB-20) cells were cultured in Hybri-Care Medium supplemented with 1.5 g/L sodium bicarbonate and 10% fetal bovine serum. MCF7 (ATCC HTB-22) cells were cultured in Minimum essential medium Eagle with Earle's Balanced Salts supplemented with 2 mM L-glutamine, 1.5 g/L sodium bicarbonate, 0.1 mM non-essential amino acids, 1.0 mM sodium pyruvate, and 10%; fetal bovine serum. T47D (ATCC HTB-133) and ZR75B (RRID: CVCL_5614) cells were cultured in RPMI-1640 Medium supplemented with 0.2 Units/ml bovine insulin and 10% fetal bovine serum. The MCF7 cells were transfected with IRG1 (ACOD1) (NM_001258406) Human Tagged ORF Clone (RG232825, OriGene Technologies, Inc.) using a TransIT®-BrCa Transfection Reagent (MIR5500, Mirus Bio LLC.) according to the manufacturer's protocol and stably transfected clones were selected by 0.2 mg/ml G418 screening.

Clonogenic assays

The breast cancer cells were seeded into 6-well plates at a density of 5×10^2 cells/well in the presence and absence of concentrations of itaconate or 4-Octyl-itaconate for 10-14 days. The cells were fixed in 4% formaldehyde overnight, stained with 0.2% crystal violet dye (1%, V5265, Sigma-Aldrich), and dissolved in 33% acetic acid before the absorbance at 595 nm with a Synergy H1 Hybrid Multi-Mode Reader (Agilent Technologies).

Immunohistochemistry (IHC)

Immunohistochemistry was performed to evaluate IRG1 expression in paraffin-embedded invasive breast carcinoma specimens. The use of human breast cancer samples was approved by the China Medical University Hospital Research Ethics Committee and complied with all relevant ethical regulations. All tissue samples were collected in compliance with the informed consent policy. The slides were stained with an IRG1 antibody (1:100, customized polyclonal antibody synthesized from ABclonal Inc.) using an automatic slide stainer BenchMark XT (Ventana Medical Systems) and counterstained with Harris hematoxylin. Two independent pathologies evaluated the slides under a light microscope. Immunoreactivity was classified by estimating the percentage (P) of tumor cells exhibiting characteristic staining (from an undetectable level, 0%, to homogeneous staining, 100%) and by estimating the intensity (I) of staining (1, weak staining; 2, moderate staining; and 3, intense staining). Results were scored by multiplying the percentage of positive cells by the intensity (i.e., quick score Q = P × I; maximum = 300) [27].

Quantitative RT-PCR (qPCR)

Total RNA was isolated using a High Pure RNA Isolation Kit (Roche). cDNA was synthesized from the isolated RNA using SuperScript™ IV First-Strand Synthesis System (Thermo Fisher Scientific Inc.). qPCR was performed with a StepOnePlus Real-Time PCR System (Thermo Fisher Scientific Inc.) using TaqMan Universal Master Mix (Thermo Fisher Scientific Inc.). All qPCR analyses were performed as both biologic and technical triplicate repeats. IRG1 (Taqman primer Hs00985781_m1) and Actin (Taqman primer Hs01060665_g1) were obtained from Thermo Fisher Scientific Inc. Relative expression of the target genes (IRG1) to the control gene (Actin) were calculated using the ΔC_T method: relative expression = $2^{-\Delta C}{}_T$, where $\Delta C_T = C_{T\,(Target)} - C_{T\,(Actin)}$.

Western blotting analysis

The cells were lysed in a RIPA buffer (50 mM Tris-HCl, pH 7.8; 150 mM NaCl; 5 mM EDTA; 5 μL/mL of Triton X-100; 5 μL/mL of NP-40; 1 μL/mL of sodium deoxycholate) and subjected to western blot analysis with the indicated antibodies. The bands were detected and revealed using fluorescent secondary antibodies, and western blot images were visualized and captured using a ChemiDoc System (Bio-Rad Laboratories, Inc.). Anti-IRG1, phospho-AMPKα1 (Thr172), and AMPKα1 were purchased from Cell Signaling Technology, Inc. Anti-Actin was purchased from Proteintech Group, Inc.

Cell cycle analysis

MCF7-GFP control and IRG1-GFP expressing cells were harvested and washed twice with cold phosphate-buffered saline (PBS) and then fixed with 70% ice-cold ethanol for 2 hours. The fixed cells were subjected to DNA content analysis using a FxCycle PI/RNase Staining Solution (Thermo Fisher Scientific Inc.) according to the manufacturer's protocol. At least 10,000 cells per sample were collected by a CytoFLEX Flow Cytometer and analyzed with CytoExpert software (Beckman Coulter Life Sciences).

DNA proliferation

MCF7 and ZR75B cells were treated with 0.5 mM itaconate or medium vehicle control for 24 hours; the cells were harvested for DNA proliferation analysis using a Click-iT EdU Alexa Fluor 594 Flow Cytometry Assay Kit (Thermo Fisher Scientific Inc.) according to the manufacturer's protocol. Briefly, the cells were treated with 10 μM EdU for 2 hours, then trypsinized and washed once with PBS and fixed in cold 70% ethanol at 4°C. At least 10,000 cells per sample were collected by a CytoFLEX Flow Cytometer and analyzed with CytoExpert software (Beckman Coulter Life Sciences).

Apoptosis assay

MCF7, T47D, and ZR75B cells were treated with 0.5 mM, 1 mM itaconate, or medium vehicle control for 48 hours, followed by harvesting with trypsin digestion for flow cytometry analysis using Annexin V Ready Flow Conjugates for Apoptosis Detection (Thermo Fisher Scientific Inc.), according to the manufacturer's protocol. At least 10,000 cells per sample were collected by a CytoFLEX Flow Cytometer and analyzed with CytoExpert software (Beckman Coulter Life Sciences). Cells without staining or stained

with annexin V-FITC or PI only were used as compensation controls.

Proteomic identification and enrichment analysis

Proteomic alterations in MCF7-GFP control and IRG1-GFP expressing cells were identified by mass spectrometric analysis (MS). Total proteins were extracted from the cells using RIPA lysis and extraction buffer (Thermo Fisher) and sonication. Protein concentrations were determined using Bio-Rad Protein Assay kits by measuring absorbance at 595 nm. Total protein samples (40 μg) were separated using 10% SDS-PAGE and divided into five gel fractions. After fine cutting (<1 mm^3), gel pieces were subjected to in-gel digestion to produce tryptic peptides. An Orbitrap Fusion mass spectrometer (Thermo Fisher Scientific) equipped with the Ultimate 3000 RSLC system (Dionex) and a nano-electrospray ion source (New Objective) were used for MS analysis. The survey scan was set at a mass range (m/z) of 375-1,500 (AGC target, 4×10^5) and a resolution of 120,000 at m/z 200. The twenty most abundant multiple-charged ions were sequentially fragmented by collision-induced dissociation for tandem mass analysis. Protein identification and label-free quantification were performed using the computational platform Proteome Discovery (v2.4). The identification threshold was set at a *P*-value <0.05. The enrichment analysis was performed using the Kyoto Encyclopedia of Genes and Genomes (KEGG) pathways with DAVID Knowledgebase v2022q4 (https://david.ncifcrf.gov/home.jsp).

Succinate dehydrogenase (SDH) activity analysis

MCF7, T47D, and ZR75B cells were treated with 1 mM itaconate or 100 μM 4-Octyl-itaconate for 24 or 48 hours. The 1×10^6 cells were homogenized in 100 μl cold SDH assay buffer, then 25 μl supernatant was taken for the following analysis using an SDH activity assay kit, according to the manufacturer's protocol.

Adenylate kinase (AK) activity analysis

2×10^6 MCF7 parental, MCF7-GFP control, IRG1-GFP expressing cells, or ZR75B cells were treated with 0, 1, or 2 mM itaconate for 24 hours, then the cells were harvested and homogenized in cold 150 μl cold AK assay buffer. 25 μg protein total cell lysate was used for AK activity assay using an AK activity assay kit (Abcam), according to the manufacturer's protocol.

ROS measurement

Various concentrations of itaconate-treated MCF7 cells were incubated with 2 μM H2DCFDA (Sigma-Aldrich Inc.) in PBS buffer for 30 min at 37°C. At least 10,000 cells per sample were collected by a CytoFLEX Flow Cytometer and analyzed with CytoExpert software (Beckman Coulter Life Sciences).

Targeted metabolites

1×10^6 GFP or IRG1-GFP MCF7 cell was collected for chemical derivatization for organic acids. Dry cell extract sample was dissolved in 35 μl of ultrapure water and added 5 μl of 0.3 M aniline/HCl (molar ratio: 5/1) and then 5 μl of 20 mg/ml 1-Ethyl-3-(3dimethyl aminopropyl)-carbodiimide (EDC). The reaction was carried out at room temperature for 2 hours and then stopped by adding 5 μl of 10% ammonium hydroxide for further 30 min incubation. The aniline-derived sample was centrifuged at 14,000 rpm for 10 min. The supernatant was subjected to LC-ESI-MS analysis of negative ion mode.

For LC-ESI-MS analysis, the LC-ESI-MS system consisted of an ultra-performance liquid chromatography (UPLC) system (ACQUITY UPLC I-Class, Waters) and an ESI/APCI source of 4 kDa quadrupole time-of-flight (TOF) mass spectrometer (Waters VION, Waters). The flow rate was set at 0.2 ml/min with column temperature at 35°C. Separation was performed with reversed-phase liquid chromatography (RPLC) on a BEH C18 column (2.1 × 100 mm, Walters) with 5 μl sample injection. The elution started from 99% mobile phase A (ultrapure water + 0.1% formic acid) and 1% mobile phase B (100% methanol + 0.1% formic acid), held at 1% B for 0.5 min, raised to 90% B in 5.5 min, held at 90% B for 1 min, and then lowered to 1% B in 1 min. The column was equilibrated by pumping 1% B for 4 min. ESI acquired LCE-SIMS chromatograms-mode under the follow-

ing conditions: capillary voltage of 2.5 kV, source temperature of 100°C, desolvation temperature at 250°C, cone gas maintained at 10 L/h, desolvation gas maintained carried at 600 L/h, and MSE mode with a range of m/z 100-1000 and 0.5 s scan time. The acquired data were processed by UNIFI software (Waters) with illustrated chromatogram and summarized in an integrated area of signals.

Lipidomic analysis

Lipids used were phosphatidylcholines, phosphatidylethanolamines, phosphatidylglycerols, phosphatidylserines, phosphatidylinositols, phosphatidic acids, sphingomyelins, diacylglycerols, triacylglycerols, fatty acids and cholesterol. The cell pellets were extracted using a Lipid Extraction Kit (Abcam) for LC-MS analysis. MS-DIAL software performed automated processing of acquired mass spectra and identifying and quantifying detected lipid species [28]. The abundance of lipids was presented as peak intensities.

Statistical analysis

All graphs present mean ± SEM from three independent assays. The Student t-test was used for experiments with two groups. ANOVA was used to compare three or more groups. A p-value of <0.05 was considered statistically significant. Statistics were performed with Prism 7.0.

Results

Itaconate inhibits breast cancer cell growth

Cancer arises through the acquisition of genetic changes, including harbor copy number variant that impacts gene dosage and drives tumorigenesis. We analyzed the genomic data from breast cancer to characterize the nature of IRG1 gene deletion ([29]; http://www.cbioportal.org). The result showed that breast cancers harboring an IRG1 deletion displayed a worse prognosis than those without IRG1 deletion, consistent with a positive correlation between the IRG1 gene expression and survival rate ([30]; Kaplan-Meier Plotter, **Figure 1A**, **1B**). Approximately 70% of breast cancer with IRG1 deletion were ER-positive (**Figure 1C**). Moreover, ER-positive breast cancer cells (BT474, MCF7, T47D, and ZR75B) were more responsive to an itaconate's derivative, 4-Octyl-itaconate (**Figure 1D**) than the ER-negative cells (Bt549, Hs578t, MAD-MB-231, and Sum159). Further, a natural IRG1's metabolic product, itaconate, also blocked the growth of ER-positive breast cancer cell lines (**Figure 1E**, **1F**). However, there was no significant difference in the IRG1 copy number, mRNA, and protein levels between ER-positive and ER-negative breast cancer cell lines and breast tumors (**Figure 1G-I**). The results suggest that itaconate may preferentially inhibit ER-positive breast cancer growth.

IRG1/Itaconate causes cell cycle arrest and apoptosis

To determine the role of endogenous itaconate in ER-positive breast cancer cells, we established an MCF7 clone with stable expression of IRG1. **Figure 2A** showed that IRG1-GFP protein was localized to mitochondria in the cells with stable IRG1 expression; in contrast, GFP protein displayed even distribution in the vector cells (**Figure 2A**, upper panels, arrowhead). Q-PCR analysis confirmed a significant increase in the level of IRG1 mRNA in IRG1-expressing cells, compared to those in vector control cells (**Figure 2B**), which was correlated with the IRG1 protein expression detected with western blot (**Figure 2C**). Importantly, mass spectrum analysis demonstrated significantly increased endogenous itaconate generation in IRG1 overexpressing cells compared to control cells (**Figure 2D**). It was noted that the cells with IRG1 expression showed significantly reduced colony numbers compared to those with the vector control, analyzed with a clonogenic assay (**Figure 2E**). Consistently, the cell cycle analysis showed that the IRG1-expressing cells caused a decreased percentage of cell numbers distributed in the S phase than the control cells (14.46% vs. 21.91%, **Figure 2F**). Simultaneously, accumulated cell numbers were distributed in the G2/M phase in the IRG1-expressing cells than the control cells (24.10% vs. 15.63%, **Figure 2F**). When measuring DNA proliferation with itaconate stimulation by a thymidine analog, Edu (5-ethynyl-2'-deoxyuridine) staining, the treated cells showed a decrease in the percentage of the stained cell number compared to those of non-treated cells (26.3% vs. 32.63% in MCF7 cells;

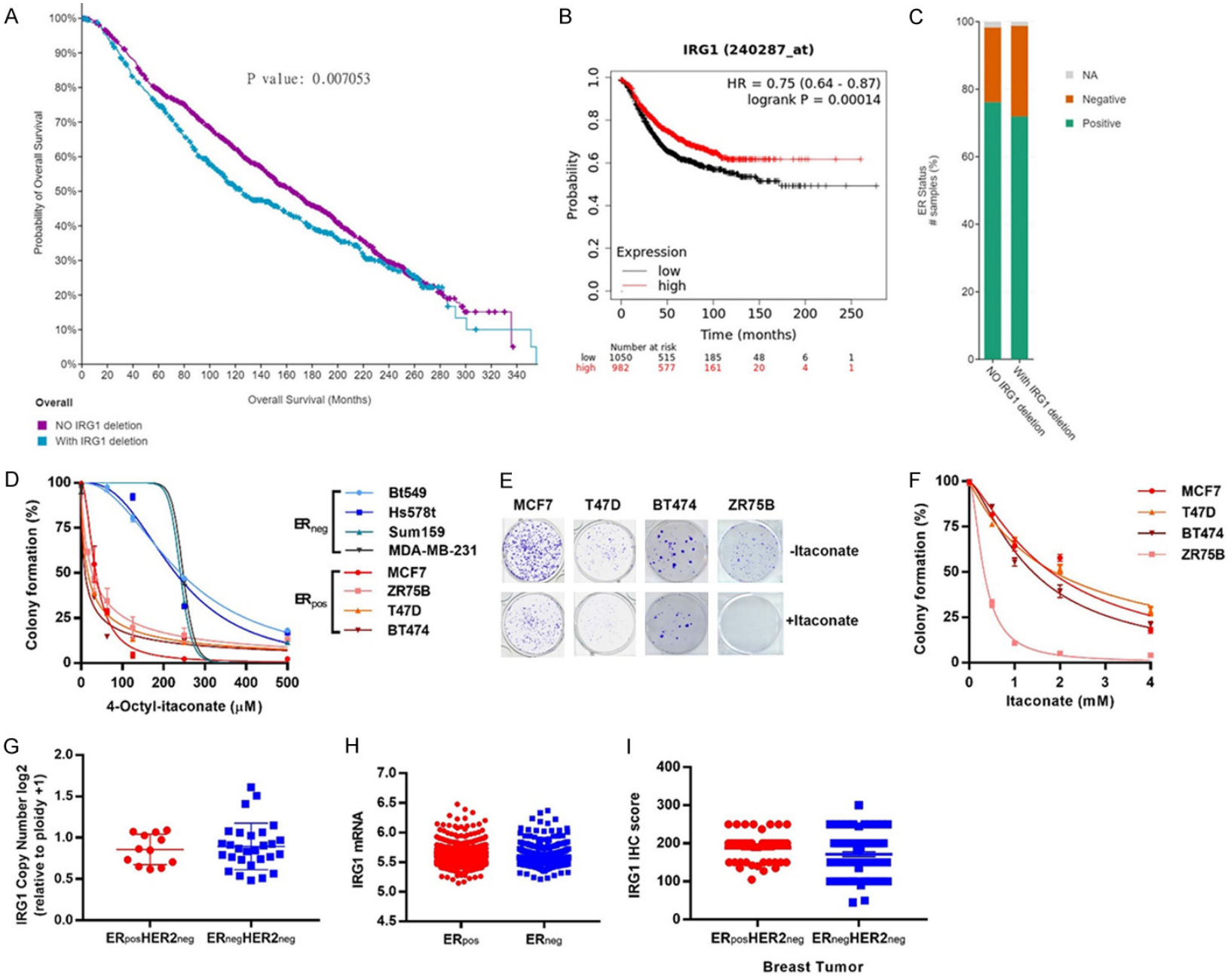
A
P value: 0.007053
Probability of Overall Survival
Overall Survival (Months)
Overall
NO IRG1 deletion
With IRG1 deletion
B
IRG1 (240287_at)
HR = 0.75 (0.64 - 0.87)
logrank P = 0.00014
Probability
Expression
low
high
Time (months)
Number at risk
low 1050 515 185 48 6 1
high 982 577 161 20 4 1
C
NA
Negative
Positive
ER Status
samples (%)
NO IRG1 deletion
With IRG1 deletion
D
Colony formation (%)
4-Octyl-itaconate (μM)
ERneg
Bt549
Hs578t
Sum159
MDA-MB-231
ERpos
MCF7
ZR75B
T47D
BT474
E
MCF7
T47D
BT474
ZR75B
-Itaconate
+Itaconate
F
MCF7
T47D
BT474
ZR75B
Colony formation (%)
Itaconate (mM)
G
IRG1 Copy Number log2
(relative to ploidy +1)
ERposHER2neg
ERnegHER2neg
H
IRG1 mRNA
ERpos
ERneg
I
IRG1 IHC score
ERposHER2neg
ERnegHER2neg
Breast Tumor

Figure 1. Itaconate suppresses ER-positive breast cancer cell growth. (A) Overall survival of breast carcinoma patients containing IRG1 deletion (blue color) as compared to those without IRG1 alteration (purple color) (http://www.cbioportal.org). (B) The correlation of survival rates with IRG1 mRNA levels in patients with breast cancer (low expression, black color vs. high expression, red color; Kaplan-Meier Plotter). All are log-rank tests. (C) ER status of breast carcinoma with or without IRG1 deletion (http://www.cbioportal.org). (D) Colony formation of various doses of 4-Octyl-itaconate-treated ER-positive (ER_{pos}) and -negative (ER_{neg}) breast cancer cells for 10-14 days. An equal volume of the medium as control. (E) Representative image and (F) Quantitative data of colony formation assay in itaconate-treated ER-positive breast cancer cells. Data are presented as mean ± SD, N = 3. (G) IRG1 copy number variation (CNV) in ER-positive ($ER_{pos}HER2_{neg}$) and ER-negative ($ER_{neg}HER2_{neg}$) breast cancer lines. The IRG1 CNVs for breast cancer cell lines were directly obtained from the Depmap portal (https://depmap.org/portal/). (H) IRG1 mRNA expressions in ER-positive (ER_{pos}) and ER-negative (ER_{neg}) breast cancer tumors. The IRG1 expression data were downloaded from the TCGA-BRCA Pan-cancer Atlas (https://www.cbioportal.org/study/summary?id=brca_tcga_pan_can_atlas_2018). (I) Detection of IRG1 by IHC in $ER_{pos}HER2_{neg}$ vs. $ER_{neg}HER2_{neg}$ breast cancer.

12.56% vs. 38.87% in ZR75B cells, **Figure 2G**). Moreover, the itaconate-treated cells underwent a dose-dependent induction of early apoptosis (**Figure 2H**). These data suggested that IRG1/Itaconate inhibited ER-positive breast cancer cell growth at least via cell cycle arrest and inducing apoptosis.

IRG1/Itaconate triggers energy stress

Itaconate is a weak competitive inhibitor of complex II-succinate dehydrogenase (SDH) of the mitochondrial electron-transport chain [18, 23, 24]. Similarly, we found that the ER-positive breast cancer cells with itaconate or 4-Octyl-itaconate stimulations showed a significant reduction in the enzymatic activity of SDH in a time-course-dependent manner (**Figure 3A**, **3B**), with the combination of reactive oxygen species (ROS) generation (**Figure 3C**). To confirm whether IRG1/Itaconate could alter energy metabolism, we measured the adenylate kinase activity, which is critical in cellular energy homeostasis by catalyzing the interconversion of ATP, ADP, and AMP [31]. Indeed, upon itaconate treatment or the condition of IRG1 expression, the cells displayed a significantly reduced enzymatic activity of adenylate kinase (AK) (**Figure 3D**, **3E**). The data supported that IRG1/Itaconate disrupted energic homeostasis by inhibiting SDH and AK, illustrated in **Figure 3F**. The conversion of cis-aconitate to itaconate by IRG1 leads to the inhibition of SDH activity, which interrupts the mitochondrial electron transport chain, and ROS production, compromising the ATP production rate and the interconversion of ATP, ADP and AMP via AK activity.

IRG1/Itaconate reprograms metabolic processes

To systematically explore the subsequent events following IRG1 activation in the ER-positive breast cancer cells, we also profiled the differential protein expression in the cells with or without IRG1 expression using label-free quantitative proteomics. Further cluster analysis with KEGG databases showed that among the 16 significantly enriched pathways, the AMPK signaling, metabolic, and glycerophospholipid pathways were the primary pathways (**Figure 4A**). Indeed, itaconate activated the AMPK signaling in the ER-positive cells by detecting an increased intensity in the AMPK phosphorylation (**Figure 4B**), consistent with the fact that the AMPK is a master regulator of metabolism that restores metabolic balance during metabolic stress [32]. For AMPK protein detection, we used the antibody which specifically recognized the catalytic subunit, AMPKα1 (MW 62 KD), and did not cross-react with AMPKα2; thus, the lower band observed in T47D cells may be the degraded form of AMPKα1 protein (approximately 47 KD).

We then further examined the change in selected intermediates of glycolysis and the TCA cycle and lipid metabolism profile, which is essential to the entire biomass and energy of the cell. When compared to control cells, IRG1 expression dampened glycolysis with a significant decrease in 1, 3-phosphoglyceric acid, phosphoenolpyruvate, and pyruvate but no significant difference in the amounts of fructose-1,6-bisphosphate and lactate. Notably, the accumulation of glyceraldehyde 3-phosphate level was seen in IRG1 cells (**Figure 4C**). The result was consistent with the previous report that itaconate modified and inhibited glyceraldehyde-3-phosphate dehydrogenase (GAPDH) activity [33], thus resulting in glyceraldehyde 3-phosphate accumulation. Also, the detectable intermediates of the TCA cycle were most decreased except succinate and malate (**Figure 4D**). Itaconate has been reported to inhibit SDH

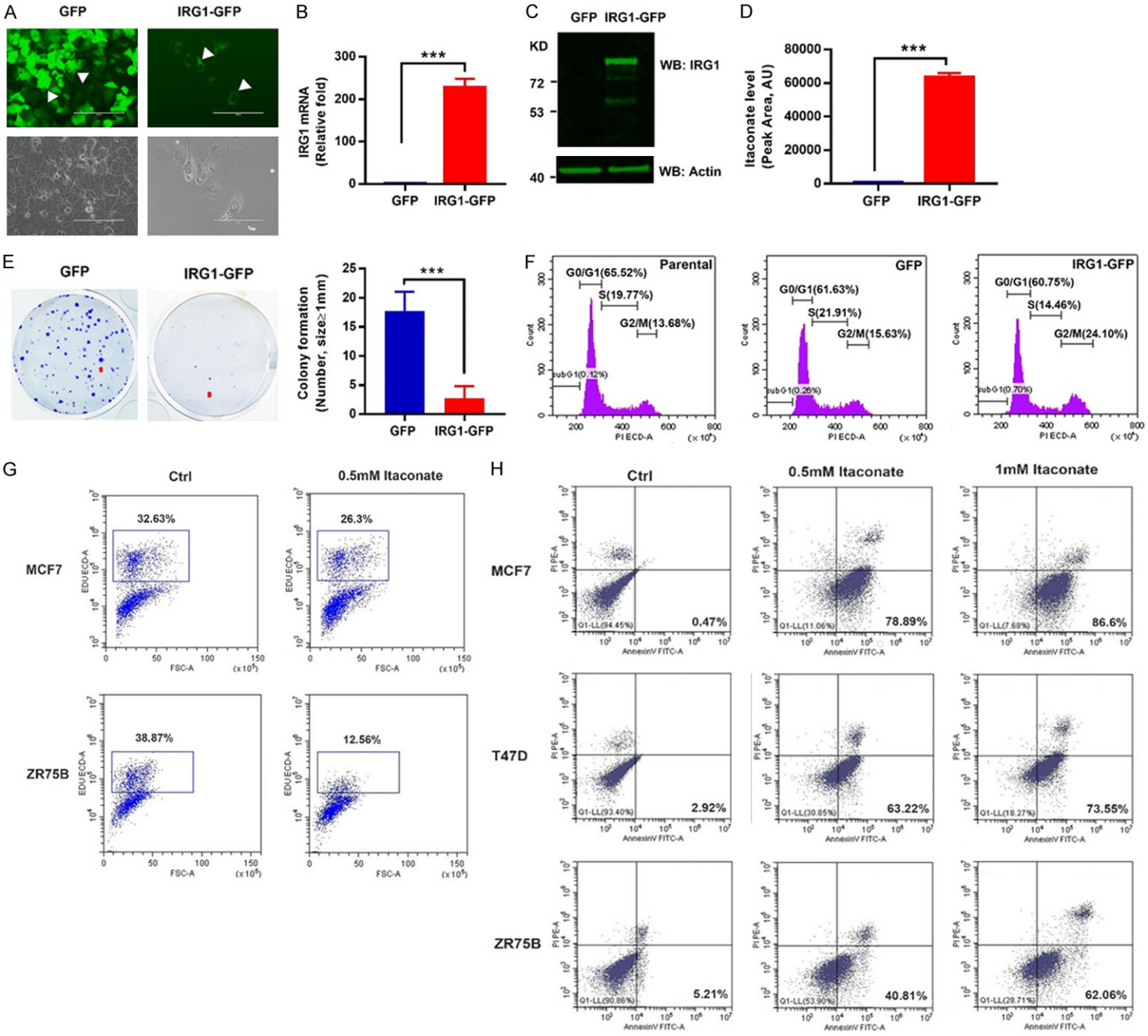
A
GFP
IRG1-GFP
B
IRG1 mRNA (Relative fold)
***
GFP
IRG1-GFP
C
GFP IRG1-GFP
KD
72
53
40
WB: IRG1
WB: Actin
D
Itaconate level (Peak Area, AU)
***
GFP
IRG1-GFP
E
GFP
IRG1-GFP
Colony formation (Number, size≥1mm)
***
GFP
IRG1-GFP
F
Parental
G0/G1(65.52%)
S(19.77%)
G2/M(13.68%)
GFP
G0/G1(61.63%)
S(21.91%)
G2/M(15.63%)
IRG1-GFP
G0/G1(60.75%)
S(14.46%)
G2/M(24.10%)
G
Ctrl
0.5mM Itaconate
MCF7
32.63%
26.3%
ZR75B
38.87%
12.56%
H
Ctrl
0.5mM Itaconate
1mM Itaconate
MCF7
0.47%
78.89%
86.6%
T47D
2.92%
63.22%
73.55%
ZR75B
5.21%
40.81%
62.06%

Figure 2. IRG1 overexpression inhibits ER-positive breast cancer cell growth. A. Representative fluorescent microscopy (upper panels) images and phase contrast (lower panels) in MCF7-IRG1-GFP vs. MCF7-GFP vector expressing cells. IRG1-GFP mitochondrial localization vs. GFP even distribution, arrowhead, scale bar 200 μm. B. Q-PCR analysis of IRG1 expression in GFP control vs. IRG1-GFP MCF7 cells. C. Western blotting analysis of IRG1 protein. D. Itaconate level (peak area) in IRG1-GFP and GFP control MCF7 cells. E. The colony formation of GFP vs. IRG1-GFP MCF7 stable cell for 14 days. Red scar bar, 1 mm. Data are presented as mean ± SD, N = 3; ***P<0.001, compared with GFP control cells. F. Cell cycle distribution histograms of parental, GFP, and IRG1-GFP MCF-7 cells. G. Dot plot of EdU-594 staining (Y-axis, 594) vs. FSC. 0.5 mM itaconate-treated MCF7 and ZR75B cells were incubated with 10 μM EdU for 2 hours. Control cells were treated with the medium. Images were acquired on a CytoFLEX Cytometer (Beckman Coulter) with cells excited using an ECD laser, and data was analyzed using CytExpert. The percentage of gated cells (EdU positive) is highlighted. H. Representative flow cytometry plots using Annexin V-FITC/PI staining for apoptosis. ER-positive breast cancer cells were treated with itaconate for 48 hours and then stained with Annexin V-FITC/PI for flow cytometric analysis.

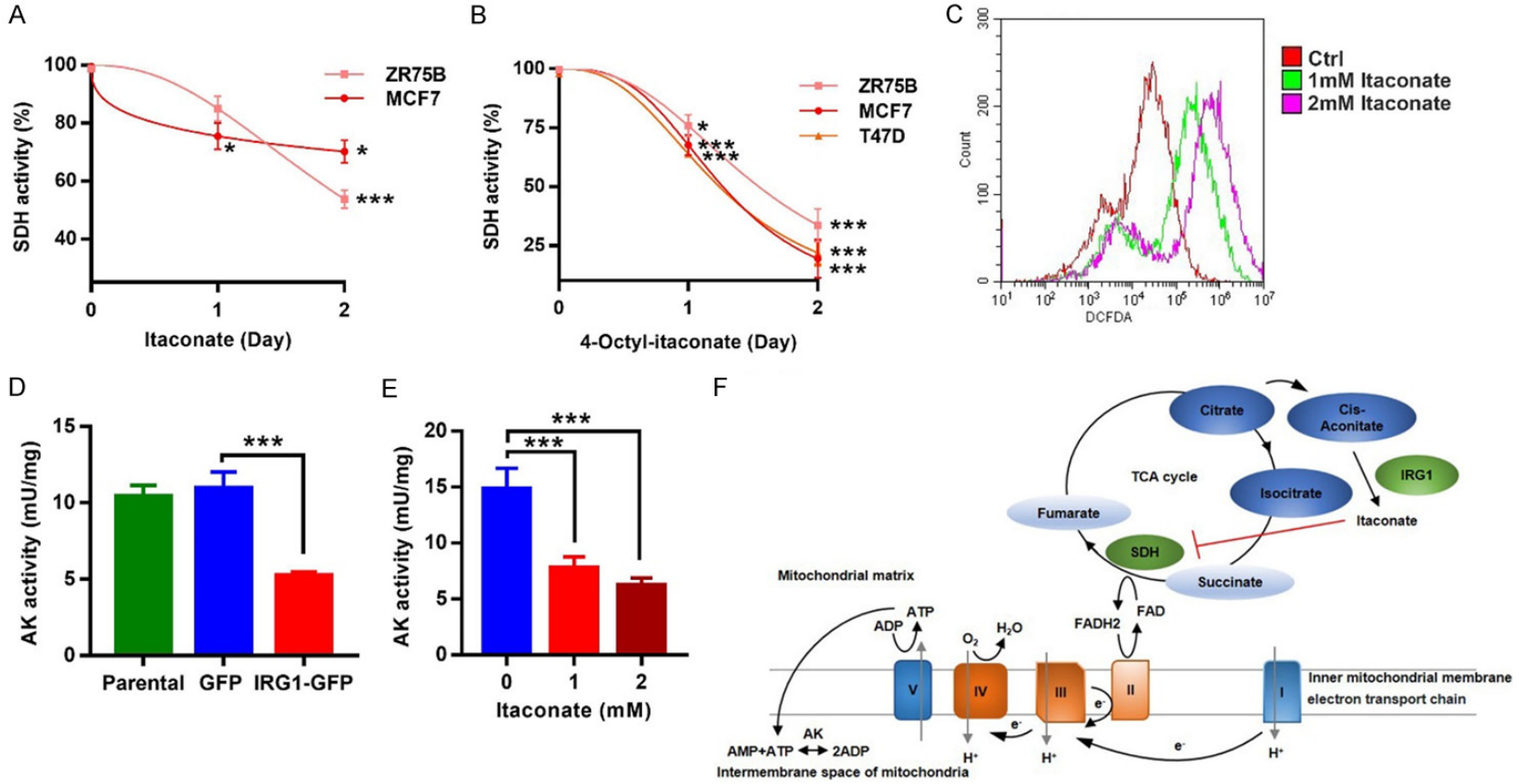

Figure 3. IRG1/Itaconate causes energy stress. Succinate dehydrogenase (SDH) activity of (A) 1 mM itaconate and (B) 100 μM 4-Octyl-itaconate treated ER-positive breast cancer cells for the indicated time, detected with an SDH activity assay kit. (C) Intracellular production of ROS in itaconate-treated MCF7 cells was measured using DCFDA, and fluorescence was measured by flow cytometry. Adenylate kinase (AK) activity of (D) GFP-control vs. IRG1-GFP MCF7 cells, and (E) Itaconate-treated ZR75B cells for 24 hours, detected with an AK activity assay kit. (F) A schematic diagram illustrates IRG1/Itaconate controlling energy homeostasis. Data are presented as mean ± SD, N = 3; *P<0.05, ***P<0.001, compared with control cells.

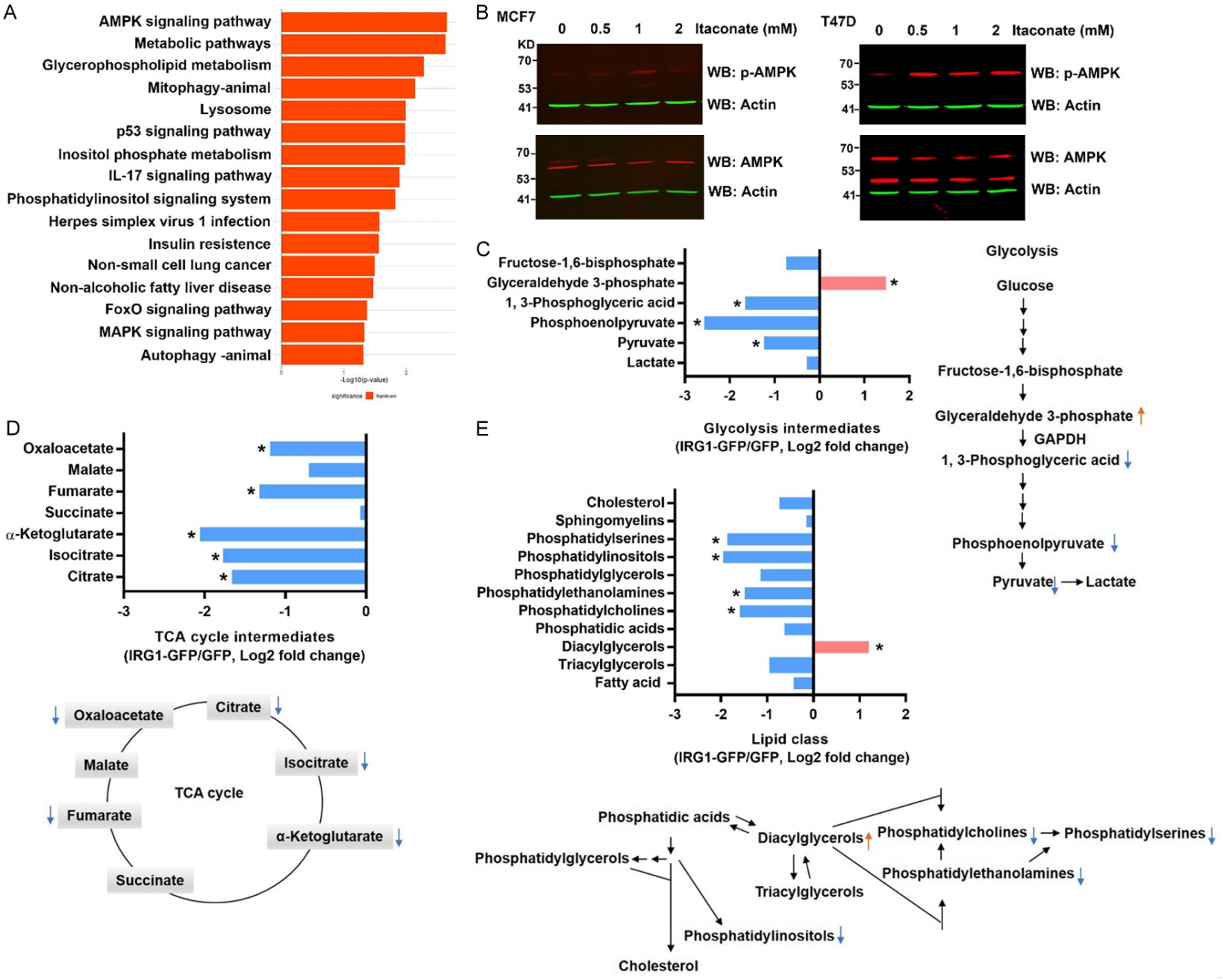
A
AMPK signaling pathway
Metabolic pathways
Glycerophospholipid metabolism
Mitophagy-animal
Lysosome
p53 signaling pathway
Inositol phosphate metabolism
IL-17 signaling pathway
Phosphatidylinositol signaling system
Herpes simplex virus 1 infection
Insulin resistence
Non-small cell lung cancer
Non-alcoholic fatty liver disease
FoxO signaling pathway
MAPK signaling pathway
Autophagy -animal
-Log10(p-value)
significance
B
MCF7
0 0.5 1 2 Itaconate (mM)
KD
70
53
41
WB: p-AMPK
WB: Actin
WB: AMPK
WB: Actin
T47D
0 0.5 1 2 Itaconate (mM)
C
Fructose-1,6-bisphosphate
Glyceraldehyde 3-phosphate
1, 3-Phosphoglyceric acid
Phosphoenolpyruvate
Pyruvate
Lactate
Glycolysis intermediates
(IRG1-GFP/GFP, Log2 fold change)
Glycolysis
Glucose
Fructose-1,6-bisphosphate
Glyceraldehyde 3-phosphate
GAPDH
1, 3-Phosphoglyceric acid
Phosphoenolpyruvate
Pyruvate
Lactate
D
Oxaloacetate
Malate
Fumarate
Succinate
α-Ketoglutarate
Isocitrate
Citrate
TCA cycle intermediates
(IRG1-GFP/GFP, Log2 fold change)
TCA cycle
E
Cholesterol
Sphingomyelins
Phosphatidylserines
Phosphatidylinositols
Phosphatidylglycerols
Phosphatidylethanolamines
Phosphatidylcholines
Phosphatidic acids
Diacylglycerols
Triacylglycerols
Fatty acid
Lipid class
(IRG1-GFP/GFP, Log2 fold change)
Phosphatidic acids
Diacylglycerols
Phosphatidylcholines
Phosphatidylserines
Phosphatidylglycerols
Phosphatidylethanolamines
Triacylglycerols
Phosphatidylinositols
Cholesterol

Figure 4. IRG1/Itaconate alters metabolic pathways. (A) Kyoto Encyclopedia of Genes and Genomes (KEGG) pathway enrichment analysis based on the differentially expressed proteins of GFP and IRG1-GFP expressing MCF7 cells ($P<0.05$). (B) Western blotting analysis of phospho-AMPK and AMPK in various concentrations of itaconate-treated ER-positive breast cancer cells. Mass spectrometry analysis of metabolites in IRG1-GFP and GFP MCF7 cells. The histograms in (C-E) show the relative amounts of intermediate metabolites of glycolysis, TCA cycle, and lipid class in IRG1 cells, respectively, compared to control cells. The bars are averages of three biological replicates yielding similar results. Significance, fold change >2.

from altering TCA cycle metabolism, causing succinate accumulation in macrophages [24, 34, 35]. However, we did not observe an increase in the level of succinate in IRG1-MCF7 cells, suggesting the effect of different cell types and cellular contexts. Phospholipids have recently attracted attention for their involvement in cancer development and drug resistance [14]; thus, we performed lipidomic analysis using mass spectrometry to gain insight into the composition of steady-state cellular lipids. We found a significant reduction in the levels of major glycerophospholipids (phosphatidylcholine, phosphatidylethanolamine, phosphatidylinositol, and phosphatidylserine) but an increment in the diacylglycerols level (**Figure 4E**). The total fatty acid, phosphatidic acids, cholesterol, sphingomyelins, triacylglycerols, and phosphatidylglycerol levels remained unchanged (**Figure 4E**). This was consistent with the proteomic data supporting that the glycerophospholipid pathway was the primary changing metabolic pathway (**Figure 4A**). In conclusion, this evidence indicated that IRG1/Itaconate results in metabolic and energy imbalance in ER-positive breast cancer cells, leading to mitochondrial dysfunction central to controlling cell viability.

Discussion

This study demonstrated that IRG1/Itaconate rewrote biochemical pathways, which resulted in increased metabolic stress from energy imbalance and inhibited ER-positive cancer cell growth. Our discoveries of the critical role of IRG1 in determining breast cancer cell fate and the potential therapeutic implication of itaconate against breast cancer may add a new dimension to the existing regulation network in breast cancer.

A previous study has suggested that the loss of 13q21-q22 is an early genetic event in breast cancer tumors without BRCA1 and BRCA2 mutations and possibly uncovers a recessive tumor suppressor gene at this locus [36]. While in the study, we showed that IRG1, located on chromosome 13q22.3, maybe a potential tumor suppressor gene via, at least in part, itaconate generation in ER-positive breast cancer cells, supporting evidence from the murine models would also be needed in the future. But, accumulated evidence has, thus far, provided a complex picture due, in part, to the different cancer types examined, particularly regarding the direct role of IRG1 in tumorigenesis. For example, a report demonstrated that IRG1 acted as an oncogene, driving glioma pathogenesis [4, 37, 38]. B16 melanoma or ID8 ovarian carcinoma cells increased IRG1 expression in tissue-resident macrophages, leading to itaconate production, oxidative stress, and subsequent protumor macrophage polarization in the tumor environment, ultimately promoting tumor progression in melanoma and ovarian cancer [4, 37, 39].

Deletion of the IRG1 gene occurs in approximately 40% of breast cancer (http://www.cbioportal.org); however, no mutations in the IRG1 gene were seen in these breast cancers. Hu man loss-of-function mutations in IRG1 gene are infrequent, which means the physiological synthesis of its enzymatic metabolite, itaconate, is vital at the population level [40]. It was noted that ER-positive cancer cells were more sensitive to itaconate than ER-negative cells, indicating a complex interaction between estrogen signaling and IRG1/Itaconate axis. Estrogen signaling regulates mitochondrial metabolism via nuclear and mitochondrial-mediated events [41-43]; its anti-inflammatory role is well-established [43, 44]. It would be interesting to address the crosstalk between IRG1/Itaconate and estrogen-estrogen receptor signaling in metabolism and inflammation during breast tumorigenesis.

IRG1 is a highly conserved gene expressed at very low levels in most cell types, but its mRNA is rapidly induced in macrophages under pro-

inflammatory conditions [15, 17-20]. Accumulated data from studies of IRG1/Itaconate in immune cell bioenergetics and responses, thus far, have suggested the potential therapeutically of itaconate in treating inflammatory diseases [45, 46]. Our work on newly defined aspects of IRG1/Itaconate in breast cancer cells further supported the universal effect of IRG1/Itaconate in glycolysis, TCA cycle, oxidative phosphorylation, and fatty acid metabolism. Notably, itaconate is a cysteine-modifying compound [19-21, 47], which highlights that there may be multiple effects of IRG1/Itaconate exerting on the modulation of breast cancer cell functions.

Changes in lipid metabolism have emerged as an essential driver of resistance to anticancer agents [14, 48]. Consistently, our work discovers the significantly changing glycerophospholipid profiles in IRG1-driven cells, suggesting IRG1/Itaconate as a novel application in treating tumors even resistant to hormone therapy. The mechanisms whereby IRG1/Itaconate modulates glycerophospholipid-derived lipid mediators in breast cancer cells and their communication with the tumor microenvironment will need further investigation.

The strategies targeting the metabolic enzymes in the glycolysis, glutaminolysis, and fatty acid synthesis pathways have also been developed or proposed [49, 50]; however, they have yet to be put into routine clinical practice [51]. This evidence reflects that discrete metabolic networks are acquired in different types of cancer and that other targets of the TCA cycle await to be identified for treating breast cancer. We demonstrated that a TCA cycle-derived metabolite, itaconate, functions as non-metabolic signals to dedicated breast cancer cell responses and fates. Our work shows promise in facilitating the design for developing more efficacious therapeutic and preventive strategies for breast cancer.

Acknowledgements

We thank the Proteomics Core Facility of the Research Center for Cancer Biology, China Medical University, Taichung, Taiwan. This work was supported by the Ministry of Science and Technology, Taiwan (MOST 108-2320-B-039-058-MY3 and MOST 111-2320-B-039-012 to HCW, MOST 110-2311-B-039-001 and MOST 111-2320-B-039-050 to XGL, NSTC 111-2639-B-039-001-ASP to MCH), and China Medical University, Taiwan (CMU110-MF-33 and CMU111-MF-39 to HCW, CMU109-YT-03 to XGL).

Disclosure of conflict of interest

None.

Address correspondence to: Drs. Hsueh-Chun Wang and Mien-Chie Hung, Graduate Institute of Biomedical Sciences, China Medical University, No. 100, Sec. 1, Jingmao Rd., Beitun Dist., Taichung, Taiwan. Tel: +886-4-22053366 Ext. 6735; Fax: +886-4-22333641; E-mail: hcwang1110@mail.cmu.edu.tw (HCW); Tel: +886-4-22057153; Fax: +886-4-22952121; E-mail: mhung@mail.cmu.edu.tw; mhung77030@gmail.com (MCH)

References

[1] Scabia V, Ayyanan A, De Martino F, Agnoletto A, Battista L, Laszlo C, Treboux A, Zaman K, Stravodimou A, Jallut D, Fiche M, Bucher P, Ambrosini G, Sflomos G and Brisken C. Estrogen receptor-positive breast cancers have patient specific hormone sensitivities and rely on progesterone receptor. Nat Commun 2022; 13: 3127.

[2] Lei JT, Anurag M, Haricharan S, Gou X and Ellis MJ. Endocrine therapy resistance: new insights. Breast 2019; 48 Suppl 1: S26-S30.

[3] Hultsch S, Kankainen M, Paavolainen L, Kovanen RM, Ikonen E, Kangaspeska S, Pietiainen V and Kallioniemi O. Association of tamoxifen resistance and lipid reprogramming in breast cancer. BMC Cancer 2018; 18: 850.

[4] Ryan DG, Murphy MP, Frezza C, Prag HA, Chouchani ET, O'Neill LA and Mills EL. Coupling Krebs cycle metabolites to signalling in immunity and cancer. Nat Metab 2019; 1: 16-33.

[5] Martinez-Reyes I and Chandel NS. Mitochondrial TCA cycle metabolites control physiology and disease. Nat Commun 2020; 11: 102.

[6] Anderson NM, Mucka P, Kern JG and Feng H. The emerging role and targetability of the TCA cycle in cancer metabolism. Protein Cell 2018; 9: 216-237.

[7] Chang LC, Chiang SK, Chen SE and Hung MC. Targeting 2-oxoglutarate dehydrogenase for cancer treatment. Am J Cancer Res 2022; 12: 1436-1455.

[8] Balaban S, Shearer RF, Lee LS, van Geldermalsen M, Schreuder M, Shtein HC, Cairns R,

Thomas KC, Fazakerley DJ, Grewal T, Holst J, Saunders DN and Hoy AJ. Adipocyte lipolysis links obesity to breast cancer growth: adipocyte-derived fatty acids drive breast cancer cell proliferation and migration. Cancer Metab 2017; 5: 1.

[9] Eliyahu G, Kreizman T and Degani H. Phosphocholine as a biomarker of breast cancer: molecular and biochemical studies. Int J Cancer 2007; 120: 1721-1730.

[10] Kothari C, Diorio C and Durocher F. The importance of breast adipose tissue in breast cancer. Int J Mol Sci 2020; 21: 5760.

[11] Wang B and Tontonoz P. Phospholipid remodeling in physiology and disease. Annu Rev Physiol 2019; 81: 165-188.

[12] van der Veen JN, Kennelly JP, Wan S, Vance JE, Vance DE and Jacobs RL. The critical role of phosphatidylcholine and phosphatidylethanolamine metabolism in health and disease. Biochim Biophys Acta Biomembr 2017; 1859: 1558-1572.

[13] Cao Y. Adipocyte and lipid metabolism in cancer drug resistance. J Clin Invest 2019; 129: 3006-3017.

[14] Saito RF, Andrade LNS, Bustos SO and Chammas R. Phosphatidylcholine-derived lipid mediators: the crosstalk between cancer cells and immune cells. Front Immunol 2022; 13: 768606.

[15] Michelucci A, Cordes T, Ghelfi J, Pailot A, Reiling N, Goldmann O, Binz T, Wegner A, Tallam A, Rausell A, Buttini M, Linster CL, Medina E, Balling R and Hiller K. Immune-responsive gene 1 protein links metabolism to immunity by catalyzing itaconic acid production. Proc Natl Acad Sci U S A 2013; 110: 7820-7825.

[16] Strelko CL, Lu W, Dufort FJ, Seyfried TN, Chiles TC, Rabinowitz JD and Roberts MF. Itaconic acid is a mammalian metabolite induced during macrophage activation. J Am Chem Soc 2011; 133: 16386-16389.

[17] Hall CJ, Boyle RH, Astin JW, Flores MV, Oehlers SH, Sanderson LE, Ellett F, Lieschke GJ, Crosier KE and Crosier PS. Immunoresponsive gene 1 augments bactericidal activity of macrophage-lineage cells by regulating beta-oxidation-dependent mitochondrial ROS production. Cell Metab 2013; 18: 265-278.

[18] Li Y, Zhang P, Wang C, Han C, Meng J, Liu X, Xu S, Li N, Wang Q, Shi X and Cao X. Immune responsive gene 1 (IRG1) promotes endotoxin tolerance by increasing A20 expression in macrophages through reactive oxygen species. J Biol Chem 2013; 288: 16225-16234.

[19] Bambouskova M, Gorvel L, Lampropoulou V, Sergushichev A, Loginicheva E, Johnson K, Korenfeld D, Mathyer ME, Kim H, Huang LH, Duncan D, Bregman H, Keskin A, Santeford A, Apte RS, Sehgal R, Johnson B, Amarasinghe GK, Soares MP, Satoh T, Akira S, Hai T, de Guzman Strong C, Auclair K, Roddy TP, Biller SA, Jovanovic M, Klechevsky E, Stewart KM, Randolph GJ and Artyomov MN. Electrophilic properties of itaconate and derivatives regulate the IkappaBzeta-ATF3 inflammatory axis. Nature 2018; 556: 501-504.

[20] Mills EL, Ryan DG, Prag HA, Dikovskaya D, Menon D, Zaslona Z, Jedrychowski MP, Costa ASH, Higgins M, Hams E, Szpyt J, Runtsch MC, King MS, McGouran JF, Fischer R, Kessler BM, McGettrick AF, Hughes MM, Carroll RG, Booty LM, Knatko EV, Meakin PJ, Ashford MLJ, Modis LK, Brunori G, Sevin DC, Fallon PG, Caldwell ST, Kunji ERS, Chouchani ET, Frezza C, Dinkova-Kostova AT, Hartley RC, Murphy MP and O'Neill LA. Itaconate is an anti-inflammatory metabolite that activates Nrf2 via alkylation of KEAP1. Nature 2018; 556: 113-117.

[21] Hooftman A, Angiari S, Hester S, Corcoran SE, Runtsch MC, Ling C, Ruzek MC, Slivka PF, McGettrick AF, Banahan K, Hughes MM, Irvine AD, Fischer R and O'Neill LAJ. The immunomodulatory metabolite itaconate modifies NLRP3 and inhibits inflammasome activation. Cell Metab 2020; 32: 468-478, e7.

[22] Daniels BP, Kofman SB, Smith JR, Norris GT, Snyder AG, Kolb JP, Gao X, Locasale JW, Martinez J, Gale M Jr, Loo YM and Oberst A. The nucleotide sensor ZBP1 and kinase RIPK3 induce the enzyme IRG1 to promote an antiviral metabolic state in neurons. Immunity 2019; 50: 64-76, e64.

[23] Cordes T and Metallo CM. Itaconate alters succinate and coenzyme a metabolism via inhibition of mitochondrial complex II and methylmalonyl-CoA mutase. Metabolites 2021; 11: 117.

[24] Cordes T, Wallace M, Michelucci A, Divakaruni AS, Sapcariu SC, Sousa C, Koseki H, Cabrales P, Murphy AN, Hiller K and Metallo CM. Immunoresponsive gene 1 and itaconate inhibit succinate dehydrogenase to modulate intracellular succinate levels. J Biol Chem 2016; 291: 14274-14284.

[25] Fischer C, Mamillapalli R, Goetz LG, Jorgenson E, Ilagan Y and Taylor HS. Bisphenol A (BPA) exposure in utero leads to immunoregulatory cytokine dysregulation in the mouse mammary gland: a potential mechanism programming breast cancer risk. Horm Cancer 2016; 7: 241-251.

[26] Wang Q, Li XL, Mei Y, Ye JC, Fan W, Cheng GH, Zeng MS and Feng GK. The anti-inflammatory drug dimethyl itaconate protects against colitis-associated colorectal cancer. J Mol Med (Berl) 2020; 98: 1457-1466.

[27] Charafe-Jauffret E, Tarpin C, Bardou VJ, Bertucci F, Ginestier C, Braud AC, Puig B, Geneix J, Hassoun J, Birnbaum D, Jacquemier J and Viens P. Immunophenotypic analysis of inflammatory breast cancers: identification of an 'inflammatory signature'. J Pathol 2004; 202: 265-273.
[28] Tsugawa H, Ikeda K, Takahashi M, Satoh A, Mori Y, Uchino H, Okahashi N, Yamada Y, Tada I, Bonini P, Higashi Y, Okazaki Y, Zhou Z, Zhu ZJ, Koelmel J, Cajka T, Fiehn O, Saito K, Arita M and Arita M. A lipidome atlas in MS-DIAL 4. Nat Biotechnol 2020; 38: 1159-1163.
[29] Cerami E, Gao J, Dogrusoz U, Gross BE, Sumer SO, Aksoy BA, Jacobsen A, Byrne CJ, Heuer ML, Larsson E, Antipin Y, Reva B, Goldberg AP, Sander C and Schultz N. The cBio cancer genomics portal: an open platform for exploring multidimensional cancer genomics data. Cancer Discov 2012; 2: 401-404.
[30] Lanczky A and Gyorffy B. Web-based survival analysis tool tailored for medical research (KMplot): development and implementation. J Med Internet Res 2021; 23: e27633.
[31] Dzeja P and Terzic A. Adenylate kinase and AMP signaling networks: metabolic monitoring, signal communication and body energy sensing. Int J Mol Sci 2009; 10: 1729-1772.
[32] Garcia D and Shaw RJ. AMPK: mechanisms of cellular energy sensing and restoration of metabolic balance. Mol Cell 2017; 66: 789-800.
[33] Qin W, Qin K, Zhang Y, Jia W, Chen Y, Cheng B, Peng L, Chen N, Liu Y, Zhou W, Wang YL, Chen X and Wang C. S-glycosylation-based cysteine profiling reveals regulation of glycolysis by itaconate. Nat Chem Biol 2019; 15: 983-991.
[34] Lampropoulou V, Sergushichev A, Bambouskova M, Nair S, Vincent EE, Loginicheva E, Cervantes-Barragan L, Ma X, Huang SC, Griss T, Weinheimer CJ, Khader S, Randolph GJ, Pearce EJ, Jones RG, Diwan A, Diamond MS and Artyomov MN. Itaconate links inhibition of succinate dehydrogenase with macrophage metabolic remodeling and regulation of inflammation. Cell Metab 2016; 24: 158-166.
[35] Nemeth B, Doczi J, Csete D, Kacso G, Ravasz D, Adams D, Kiss G, Nagy AM, Horvath G, Tretter L, Mocsai A, Csepanyi-Komi R, Iordanov I, Adam-Vizi V and Chinopoulos C. Abolition of mitochondrial substrate-level phosphorylation by itaconic acid produced by LPS-induced Irg1 expression in cells of murine macrophage lineage. FASEB J 2016; 30: 286-300.
[36] Kainu T, Juo SH, Desper R, Schaffer AA, Gillanders E, Rozenblum E, Freas-Lutz D, Weaver D, Stephan D, Bailey-Wilson J, Kallioniemi OP, Tirkkonen M, Syrjakoski K, Kuukasjarvi T, Koivisto P, Karhu R, Holli K, Arason A, Johannesdottir G, Bergthorsson JT, Johannsdottir H, Egilsson V, Barkardottir RB, Johannsson O, Haraldsson K, Sandberg T, Holmberg E, Gronberg H, Olsson H, Borg A, Vehmanen P, Eerola H, Heikkila P, Pyrhonen S and Nevanlinna H. Somatic deletions in hereditary breast cancers implicate 13q21 as a putative novel breast cancer susceptibility locus. Proc Natl Acad Sci U S A 2000; 97: 9603-9608.
[37] Wu R, Chen F, Wang N, Tang D and Kang R. ACOD1 in immunometabolism and disease. Cell Mol Immunol 2020; 17: 822-833.
[38] Pan J, Zhao X, Lin C, Xu H, Yin Z, Liu T and Zhang S. Immune responsive gene 1, a novel oncogene, increases the growth and tumorigenicity of glioma. Oncol Rep 2014; 32: 1957-1966.
[39] Weiss JM, Davies LC, Karwan M, Ileva L, Ozaki MK, Cheng RY, Ridnour LA, Annunziata CM, Wink DA and McVicar DW. Itaconic acid mediates crosstalk between macrophage metabolism and peritoneal tumors. J Clin Invest 2018; 128: 3794-3805.
[40] Chen F, Lukat P, Iqbal AA, Saile K, Kaever V, van den Heuvel J, Blankenfeldt W, Bussow K and Pessler F. Crystal structure of cis-aconitate decarboxylase reveals the impact of naturally occurring human mutations on itaconate synthesis. Proc Natl Acad Sci U S A 2019; 116: 20644-20654.
[41] Klinge CM. Estrogenic control of mitochondrial function and biogenesis. J Cell Biochem 2008; 105: 1342-1351.
[42] Klinge CM. Estrogenic control of mitochondrial function. Redox Biol 2020; 31: 101435.
[43] Giraud SN, Caron CM, Pham-Dinh D, Kitabgi P and Nicot AB. Estradiol inhibits ongoing autoimmune neuroinflammation and NFkappaB-dependent CCL2 expression in reactive astrocytes. Proc Natl Acad Sci U S A 2010; 107: 8416-8421.
[44] Qureshi R, Picon-Ruiz M, Aurrekoetxea-Rodriguez I, Nunes de Paiva V, D'Amico M, Yoon H, Radhakrishnan R, Morata-Tarifa C, Ince T, Lippman ME, Thaller SR, Rodgers SE, Kesmodel S, Vivanco MDM and Slingerland JM. The major pre- and postmenopausal estrogens play opposing roles in obesity-driven mammary inflammation and breast cancer development. Cell Metab 2020; 31: 1154-1172, e9.
[45] Lin J, Ren J, Gao DS, Dai Y and Yu L. The emerging application of itaconate: promising molecular targets and therapeutic opportunities. Front Chem 2021; 9: 669308.
[46] Hooftman A and O'Neill LAJ. The immunomodulatory potential of the metabolite itaconate. Trends Immunol 2019; 40: 687-698.
[47] Bambouskova M, Potuckova L, Paulenda T, Kerndl M, Mogilenko DA, Lizotte K, Swain A, Hayes S, Sheldon RD, Kim H, Kapadnis U, Ellis

AE, Isaguirre C, Burdess S, Laha A, Amarasinghe GK, Chubukov V, Roddy TP, Diamond MS, Jones RG, Simons DM and Artyomov MN. Itaconate confers tolerance to late NLRP3 inflammasome activation. Cell Rep 2021; 34: 108756.

[48] Pitroda SP, Khodarev NN, Beckett MA, Kufe DW and Weichselbaum RR. MUC1-induced alterations in a lipid metabolic gene network predict response of human breast cancers to tamoxifen treatment. Proc Natl Acad Sci U S A 2009; 106: 5837-5841.

[49] Gandhi N and Das GM. Metabolic reprogramming in breast cancer and its therapeutic implications. Cells 2019; 8: 89.

[50] Hart CD, Tenori L, Luchinat C and Di Leo A. Metabolomics in breast cancer: current status and perspectives. Adv Exp Med Biol 2016; 882: 217-234.

[51] Long JP, Li XN and Zhang F. Targeting metabolism in breast cancer: how far we can go? World J Clin Oncol 2016; 7: 122-130.